

SLIDER-CRANK MECHANISM MODELLING WITH CLEARANCE IN PISTON-PIN REVOLUTE JOINT

Vitor L. Reis*¹, Katia L. Cavalca¹

¹Univesity of Campinas
vreis88@gmail.com
katia@fem.unicamp.br

Keywords: slider-crank mechanism, piston-pin, revolute clearance joint, hydrodynamic lubrication, Hertz contact model, Coulomb friction.

Abstract. *This work presents a comparison of different lubrication models for the slider-crank mechanism with clearance on the piston-pin revolute joint. The equations of motion for this system are obtained by Lagrange's method and the effects related to contact, friction and lubrication at the elements that operate in the clearance are considered in the model. The contact force model used in this work is based on Hertz formulation, considering the inclusion of the dissipative effect associated with the impact between the pin and the hole of the slider. The frictional force adopted is based on the Coulomb friction but adapted to the multi-body dynamics approach. Two models of hydrodynamic lubrication are compared: the Pinkus' model applied in the literature and the Bannwart's model considering the effect of the acceleration of the lubricant fluid imposed on the movement of the mechanism. It was observed that the models don't guarantee the support of the pin-piston system for hydrodynamic lubrication approach. Based on comparison with previous works, the model proposed here is promising to foresee the next steps for reproducing the behavior of the dynamics of the revolute joint with clearance.*

1 INTRODUCTION

The slider-connecting rod joint is characterized as a revolute joint, highly applied in slider-crank mechanisms similar to the piston-pin joint in combustion engines. However, as it involves an oscillatory motion, the lubrication model applied to this kind of joint must be carefully investigated when the clearance is considered in the joint. In this case, the clearance is filled with a lubricant that generates a pressure distribution and, consequently, hydrodynamic forces actuating in the components of the mechanical system. Some authors have been investigating the dynamic behaviour of mechanisms considering the lubrication at the clearance joints.

Schwab et al. [1] compared different revolute joint clearance models in the dynamic analysis of rigid and elastic mechanical systems. The hydrodynamic lubrication model, in this case, considered the finite length of the bearing and the effect of cavitation in the fluid film.

In 2004, Flores et al. [2] accomplished a dynamic analysis of a mechanical system with lubricated joints, applying a hydrodynamic lubrication model to an infinitely long journal bearing, taking into account the hydrodynamic forces due to only squeeze effects. However, for high angular velocities, the simple squeeze approach is not valid and, consequently, the Reynolds equation should be applied. Flores et al. [3] continued the study on dynamics of mechanical systems including joints with clearance with a hydrodynamic lubrication model based on the solution of the Reynolds equation, considering the infinitely long journal bearing condition, besides squeeze and wedge effects.

In 2009, Flores et al. [4] presented a general methodology for the lubricated revolute joints modelling in constrained rigid multibody systems.

Tian et al. [5] simulated the behavior of planar flexible multibody systems with clearance and lubricated revolute joints. For lubricated revolute joints, the hydrodynamic forces were calculated as proposed by Flores et al. [4]. However, aiming to consider possible cavitation effects, some modifications were done in the lubrication model as proposed by Ravn et al. [6].

Daniel and Cavalca [7] analyzed the dynamic of a slider–crank mechanism with hydrodynamic lubrication in the connecting rod–slider joint clearance. The hydrodynamic lubrication model was previously developed by Bannwart et al. [8] and it considered the infinitely long journal bearing condition. The hydrodynamic forces were obtained due to wedge effects.

Finally, Machado et al. [9] studied the effect of the lubricated revolute joint parameters and hydrodynamic force models on the dynamic response of planar multibody systems. This way, three different hydrodynamic force models were considered, being the Pinkus and Sternlicht [10] model for infinitely long journal-bearings and the Frêne et al. [11] models for infinitely long and short journal-bearings. According the results obtained in the simulations, the hydrodynamic force models changed the dynamic characteristics of the multibody systems. Therefore, the lubrication model applied in the piston-pin system analysis should be carefully chosen.

2 DYNAMICAL MODEL OF THE MECHANISM

A planar slider-crank mechanism is shown in Figure 1. This mechanism is widely used in machines like internal combustion engines and it is modelled to have a revolute joint clearance at the slider. This cylindrical joint attaches the connecting rod pin (in black) to the slider. The mechanism has three degrees of freedom (or independent co-ordinates): the crank angular displacement (q); the connecting rod angular displacement (A) and the slider horizontal position (X_{PT}).

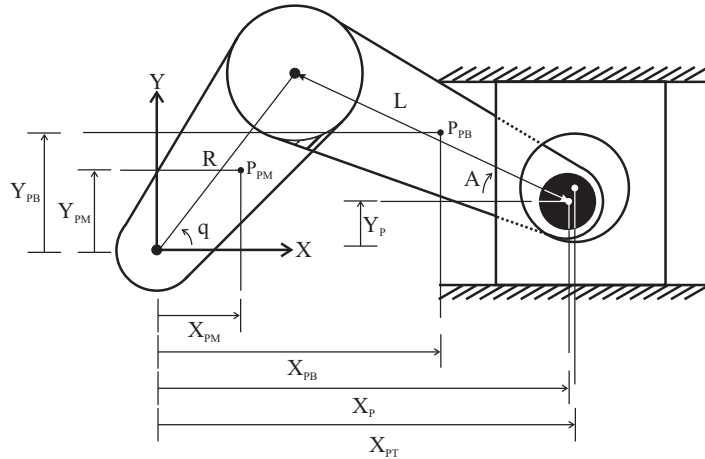


Figure 1: Slider-crank mechanism.

From Figure 1, the following geometric parameters are defined: the crank length (R); and the length of the connecting rod (L). The position of the center of pin (X_p, Y_p) and its velocity at inertial frame (\dot{X}_p, \dot{Y}_p) is calculated from expressions (1) and (2) respectively [12].

$$\begin{Bmatrix} \dot{X}_p \\ \dot{Y}_p \end{Bmatrix} = \begin{Bmatrix} R\cos(q) + L\cos(A) \\ R\sin(q) - L\sin(A) \end{Bmatrix} \quad (1)$$

$$\begin{Bmatrix} \dot{X}_p \\ \dot{Y}_p \end{Bmatrix} = \begin{bmatrix} -R\sin(q) & -L\sin(A) \\ R\cos(q) & -L\cos(A) \end{bmatrix} \begin{Bmatrix} \dot{q} \\ \dot{A} \end{Bmatrix} \quad (2)$$

In order to evaluate the equation of motion of the subsystem composed by the crank and the connecting rod, a kinematic analysis of the centre of mass of these bodies is required. Figure 2 shows the position of these points of interest on each component of the subsystem and the coupling loads that arise from the modelling of the clearance.

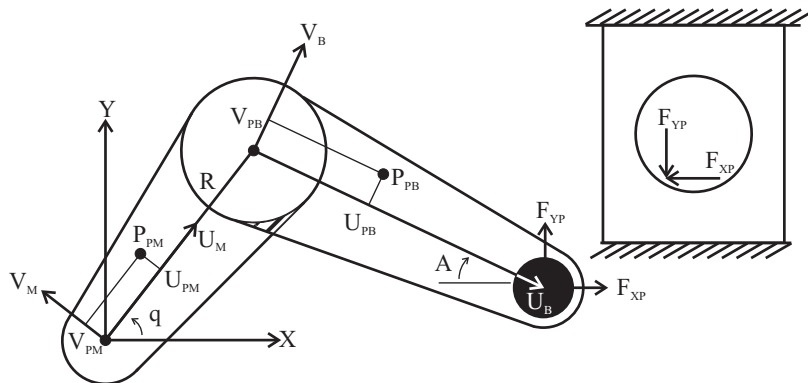


Figure 2: Subsystems with centers of masses and coupling loads applied in the mechanism.

According to Figure 2, U_{PM} and V_{PM} are the mass center coordinates of the crank (P_{PM}) in the referential system located in the crank (U_M, V_M), U_{PB} and V_{PB} are the centre of mass coordinates of the connecting rod (P_{PB}) in the reference frame located in the connecting rod (U_B, V_B), X_{PM} and Y_{PM} are the linear displacements of the center of mass of the crank (P_{PM}) in the inertial referential system (X, Y) and X_{PB} and Y_{PB} are the linear displacements of the center of mass of the connecting rod (P_{PB}) in the inertial referential system (X, Y) [12].

The position for the crank center of mass is:

$$\begin{Bmatrix} X_{PM} \\ Y_{PM} \end{Bmatrix} = \begin{Bmatrix} U_{PM}\cos(q) - V_{PM}\sin(q) \\ U_{PM}\sin(q) + V_{PM}\cos(q) \end{Bmatrix} \quad (3)$$

Analogously, the position of the connecting rod centre of mass is:

$$\begin{Bmatrix} X_{PB} \\ Y_{PB} \end{Bmatrix} = \begin{Bmatrix} R\cos(q) + U_{PB}\cos(A) + V_{PB}\sin(A) \\ R\sin(q) - U_{PB}\sin(A) + V_{PB}\cos(A) \end{Bmatrix} \quad (4)$$

Figure 2 also presents the coupling (F_{xp} and F_{yp}) forces applied to the mechanism. The generalized components of the force applied on the subsystem crank-connecting rod are:

$$\begin{Bmatrix} Q_q \\ Q_A \end{Bmatrix} = \begin{Bmatrix} F_{yp}R\cos(q) - F_{xp}R\sin(q) \\ -F_{yp}L\cos(A) - F_{xp}L\sin(A) \end{Bmatrix} \quad (5)$$

The slider equation of motion is obtained by the force balance, resulting in:

$$M_{PT}\ddot{X}_{PT} = -(F_{ext} + F_{xp}) \quad (6)$$

Defining I_{M0} e I_B as the crank rotational inertia in relation to inertial reference frame, and connecting rod rotational inertia, the complete equation of motion (7) for this mechanism with clearance is obtained applying the second form of Lagrange Method [7,12].

$$\begin{bmatrix} M_B R^2 + I_{M0} & -M_B R(U_{PB}\cos(A+q) + V_{PB}\sin(A+q)) \\ \text{sym} & M_B(U_{PB}^2 + V_{PB}^2) + I_B \end{bmatrix} \begin{Bmatrix} \ddot{q} \\ \ddot{A} \end{Bmatrix} + M_B R(V_{PB}\cos(A+q) - U_{PB}\sin(A+q)) \begin{bmatrix} \dot{q}^2 & 0 \\ 0 & \dot{A}^2 \end{bmatrix} = \begin{Bmatrix} F_{yp}R\cos(q) - F_{xp}R\sin(q) \\ -F_{yp}L\cos(A) - F_{xp}L\sin(A) \end{Bmatrix} \quad (7)$$

$$M_{PT}\ddot{X}_{PT} = -(F_{ext} + F_{xp})$$

2.1 Relative motion between connecting rod and piston

The equation of motion obtained in the last section presents the typical case of coupling in multibody system with clearances. In such systems the kinematic constraints are replaced by force constraints (e.g. F_{xp} and F_{yp}). The evaluation of the magnitude of these forces and their directions are based on relative motion between the connecting rod and the piston [2].

Defining the radial clearance (c_r) as the difference between the journal radius (pin) and the bearing radius (hole on the slider), and the relative distance between their centers position as eccentricity vector (\vec{e}), it's possible to determine if these bodies are in contact or not.

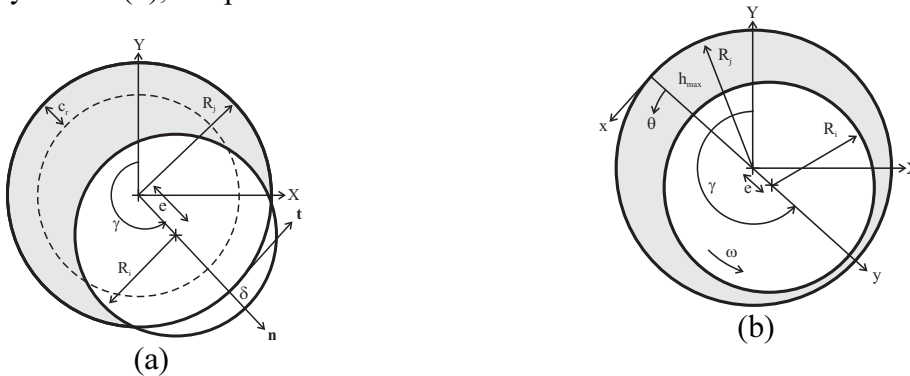


Figure 3: Contact (a) and Lubrication (b) representations.

According to Figures 1 and 3(a) the components of the eccentricity vector are calculated as:

$$e = \begin{Bmatrix} e_x \\ e_y \end{Bmatrix} = \begin{Bmatrix} X_p - X_{PT} \\ Y_p - Y_{PT} \end{Bmatrix} \quad (8)$$

When the impact occurs, the normal penetration depth δ is calculated as:

$$\delta = e - c_r \quad (9)$$

The eccentricity ratio (ε) is defined as the ratio of eccentricity by radial clearance:

$$\varepsilon = \frac{e}{c_r} \quad (10)$$

The time rate of eccentricity ratio variation, denoted by $\dot{\varepsilon}$, is obtained by differentiating the expression (10) with respect to time:

$$\dot{\varepsilon} = \frac{\dot{e}}{c_r} \quad (11)$$

The γ angle, shown in Figure 3(a), is calculated as:

$$\gamma = \text{atan2} \left(\frac{e_y}{e_x} \right) \quad (12)$$

And its derivate with respect to time is calculated as follows:

$$\dot{\gamma} = \frac{e_x \dot{e}_y - e_y \dot{e}_x}{e^2} \quad (13)$$

To calculate the relative velocities in which the bodies interact, it's necessary to find the point along the eccentricity line where the process of contact occurs. The position of this point is calculated as follows:

$$\begin{aligned} X_k^c &= X_k + R_k \cos(\gamma) \\ Y_k^c &= Y_k + R_k \sin(\gamma) \end{aligned} \quad k = i, j \quad (14)$$

Where R_i and R_j represents the journal and the bearing radius. The velocity of the point of contact is calculated as:

$$\begin{aligned} \dot{X}_k^c &= \dot{X}_k - \dot{\gamma} R_k \sin(\gamma) \\ \dot{Y}_k^c &= \dot{Y}_k + \dot{\gamma} R_k \cos(\gamma) \end{aligned} \quad k = i, j \quad (15)$$

And the relative scalar velocities of these bodies are:

$$\begin{aligned} \dot{X}_{rel}^c &= \dot{X}_j^c - \dot{X}_i^c \\ \dot{Y}_{rel}^c &= \dot{Y}_j^c - \dot{Y}_i^c \end{aligned} \quad (16)$$

Finally the relative normal and tangential velocities to the plane of collision are calculated:

$$\begin{aligned} v_N &= \dot{X}_{rel}^c \cos(\gamma) + \dot{Y}_{rel}^c \sin(\gamma) \\ v_T &= -\dot{X}_{rel}^c \sin(\gamma) + \dot{Y}_{rel}^c \cos(\gamma) \end{aligned} \quad (17)$$

3 CONTACT AND FRICTION'S FORCE MODELS

The contact force model used in this application was proposed by Lankarani and Nikravesh [13]. This model is widely used in mechanical simulations of multibody mechanisms with clearances [14]. In this model the contact force includes a dissipative term, proportional to the impact velocity of the bodies, and although it has been developed for spheres collision, it is

commonly used for cylindrical contact [14]. According to this formulation, the normal force acting on the bodies in contact is:

$$F_N = K\delta^n + D\dot{\delta} \quad (18)$$

where δ is the indentation, the exponent n depends on the of materials in contact, $\dot{\delta}$ is the relative normal velocity of the bodies and K is the contact stiffness obtained by:

$$K = \frac{4}{3(\sigma_i + \sigma_j)} \left[\frac{R_i R_j}{R_i + R_j} \right]^{\frac{1}{2}} \quad (19)$$

The parameter σ_k is calculated as follows:

$$\sigma_k = \frac{1 - \nu^2}{E_k} \left[\frac{R_i R_j}{R_i + R_j} \right]^{\frac{1}{2}} \quad k = i, j \quad (20)$$

with ν being the Poisson ratio and E the Young modulus of the materials in contact. The parameter D that controls the dissipation energy in the contact is obtained by:

$$D = \frac{3K(1 - c_e)^2}{4\dot{\delta}^{(-)}} \delta^n \quad (21)$$

where c_e is the restitution coefficient and $\dot{\delta}^{(-)}$ is the impact velocity. The final expression for normal contact force is:

$$F_N = K\delta^n \left[1 + \frac{3(1 - c_e)^2}{4} \frac{\dot{\delta}}{\dot{\delta}^{(-)}} \right] \quad (22)$$

The friction force model used in the simulations is based on Coulomb friction theory [15], expressed as follows:

$$F_T = -c_f c_d F_N \frac{v_T}{v_T} \quad c_d = \begin{cases} 0 & \text{if } v_T < v_0 \\ \frac{v_T - v_0}{v_1 - v_0} & \text{if } v_0 < v_T < v_1 \\ 1 & \text{if } v_T > v_1 \end{cases} \quad (23)$$

In which c_f is a friction coefficient, c_d is a dynamic coefficient dependent on the relative velocity of sliding between two bodies. The v_T is a tangential velocity and v_T is its modulus and v_0 and v_1 are the given tolerances for sliding velocity.

4 LUBRICATION'S MODELS

This paper proposes an investigation of two lubrication models. The first model reports to Pinkus and Sternlicht [10] and it was applied in recent papers [4, 9] dealing with multibody systems. This formulation takes into account the relative motion between the journal and the bearing, and it also considers the squeeze and the wedge effects.

In Figure 3b the reference frame for the hydrodynamic bearing analysis is presented. Defining ω as the angular velocity of the journal in the counterclockwise, the relations given by Eq. (24) are established:

$$E = \frac{2}{\omega} \dot{\epsilon} \quad G = \frac{2}{\omega} \dot{\gamma} \quad (24)$$

These relations are used in the Reynolds equation, and the expressions of the forces applied on the journal are evaluated in details in reference [10]. For positive values of E , the resultant forces in the local frame (x,y) are:

$$\begin{cases} F_y \\ F_x \end{cases} = \begin{cases} -\frac{1}{2} \frac{\mu \omega R_j^3}{c_r^2} \frac{3E}{(2 + \varepsilon^2)(1 - \varepsilon^2)(1 - \varepsilon^2)^{0.5}} \left[4k\varepsilon^2 + (2 + \varepsilon^2)\pi \frac{k+3}{k+3/2} \right] \\ -\frac{1}{2} \frac{\mu \omega R_j^3}{c_r^2} \frac{6\pi\varepsilon(1-G)}{(2 + \varepsilon^2)(1 - \varepsilon^2)^{0.5}} \left(\frac{k+3}{k+3/2} \right) \end{cases} \quad (25)$$

For negative values of E the forces in the local frame are:

$$\begin{cases} F_y \\ F_x \end{cases} = \begin{cases} +\frac{1}{2} \frac{\mu \omega R_j^3}{c_r^2} \frac{3E}{(2 + \varepsilon^2)(1 - \varepsilon^2)(1 - \varepsilon^2)^{0.5}} \left[4k\varepsilon^2 - (2 + \varepsilon^2)\pi \frac{k}{k+3/2} \right] \\ -\frac{1}{2} \frac{\mu \omega R_j^3}{c_r^2} \frac{6\pi\varepsilon(1-G)}{(2 + \varepsilon^2)(1 - \varepsilon^2)^{0.5}} \left(\frac{k}{k+3/2} \right) \end{cases} \quad (26)$$

where k is defined by:

$$k = (1 - \varepsilon^2)^{0.5} \left[\left(\frac{1-G}{E} \right)^2 + \frac{1}{\varepsilon^2} \right]^{0.5} \quad (27)$$

The resultant forces are written in the inertial frame (X,Y) applying the following coordinate transformation:

$$\begin{cases} F_Y \\ F_X \end{cases} = \begin{cases} F_y \sin(\gamma) - F_x \cos(\gamma) \\ F_y \cos(\gamma) + F_x \sin(\gamma) \end{cases} \quad (28)$$

The second lubrication model considers the alternating rotational motion in the journal bearing of the connecting rod-slider joint and the motion of the bearing fixed in the slider [8]. In this case, the tangential (angular) and radial velocities in the oil film have an imaginary part due to the oscillating motion of the connecting rod pin in both directions [7, 8]. This lubrication model assumes that the fluid velocity in the axial coordinate is practically nil, as an infinitely long bearing. Moreover, the fluid is considered incompressible and Gumbel's cavitation condition is considered. Therefore, the velocity field presented in this model is obtained from Eq.(29).

$$V_\theta(y, \theta) = \frac{U_0 \sinh \left(h(\theta) - y \sqrt{\frac{i\dot{q}}{\nu}} \right)}{\sinh \left(h(\theta) \sqrt{\frac{i\dot{q}}{\nu}} \right)} + \frac{\nu}{i\dot{q}\mu R_i} \frac{dP_t}{d\theta} \left\{ \frac{\sinh \left(h(\theta) - y \sqrt{\frac{i\dot{q}}{\nu}} \right) + \sinh \left(y \sqrt{\frac{i\dot{q}}{\nu}} \right)}{\sinh \left(h(\theta) \sqrt{\frac{i\dot{q}}{\nu}} \right)} - 1 \right\} \quad (29)$$

The variables U_0 , \dot{q} , R_i , h , ν and μ are the linear velocity in the shaft surface, rotational speed of the crank, bearing radius, fluid film thickness, kinematic viscosity, and absolute viscosity, respectively. Considering the condition $P(0) = P(2\pi) = P_0$, the pressure distribution is presented as:

$$P(\theta) = P_0 + \rho \dot{q} R_i U_0 \left\{ \frac{L}{R_i} [1 - \cos(\theta)] - \theta i \right\} + \mu R_i U_0 \frac{i\dot{q}}{\nu} \int_0^\theta \frac{\tanh \left[\frac{h(\theta)}{2} \sqrt{\frac{i\dot{q}}{\nu}} \right] - K_1 \frac{c_r}{2} \sqrt{\frac{i\dot{q}}{\nu}}}{h(\theta) \sqrt{\frac{i\dot{q}}{\nu}} - 2 \tanh \left[\frac{h(\theta)}{2} \sqrt{\frac{i\dot{q}}{\nu}} \right]} d\theta \quad (30)$$

where ρ is the oil density and K_1 is defined as:

$$K_1 = \int_0^{2\pi} \left\{ \frac{\tanh \left[\frac{h(\theta)}{2} \sqrt{\frac{i\dot{q}}{v}} \right]}{h(\theta) \sqrt{\frac{i\dot{q}}{v}} - 2 \tanh \left[\frac{h(\theta)}{2} \sqrt{\frac{i\dot{q}}{v}} \right]} - 1 \right\} d\theta \Bigg/ \frac{c_r}{2} \sqrt{\frac{i\dot{q}}{v}} \int_0^{2\pi} \frac{d\theta}{h(\theta) \sqrt{\frac{i\dot{q}}{v}} - 2 \tanh \left[\frac{h(\theta)}{2} \sqrt{\frac{i\dot{q}}{v}} \right]} \quad (31)$$

Finally, the hydrodynamic forces of the fluid film acting on the journal ($y = h$) are:

$$F_x = wR_j \int_0^{2\pi} \left(-P \sin(\theta) + \mu \frac{\partial V_\theta}{\partial y} \cos(\theta) \right)_{y=h} d\theta \quad (32)$$

$$F_y = wR_j \int_0^{2\pi} \left(-P \cos(\theta) + \mu \frac{\partial V_\theta}{\partial y} \sin(\theta) \right)_{y=h} d\theta \quad (33)$$

Both models cover the hydrodynamic lubrication condition, and when a transition from lubrication to contact occurs, the pressure developed in a fluid film approaches to a Hertzian contact pressure distribution. In order to minimize effects of a rough transition between lubrication and contact, a scheme presented in Eq. (34) is used [2, 4].

$$F = \begin{cases} F_{\text{lubricated}} & \text{if } e \leq c_r \\ \frac{(c_r + e_0) - e}{e_0} F_{\text{lubricated}} + \frac{e - c_r}{e_0} F_{\text{dry}} & \text{if } c_r \leq e \leq c_r + e_0 \\ F_{\text{dry}} & \text{if } e \geq c_r + e_0 \end{cases} \quad (34)$$

According to Eq. (34), the system is in hydrodynamic lubrication up to the radial clearance c_r , and the hybrid lubrication condition (hydrodynamic + dry) is calculated considering the radial clearance boundary as $c_r + e_0$, which is the starting point to the dry contact transition.

However, to guarantee the continuity in the force evaluation (avoiding jumps to infinite values) the radial clearance used in the forces evaluation is $c_r + e_0 + e_1$, where e_0 and e_1 are given tolerances to eccentricity, carefully chosen as function of radial clearance.

The dynamic equations developed in the last sections were integrated in time, using a Predictor-Corrector integrator, developed by Shampine and Gordon [16], largely applied in dynamic simulations of nonlinear systems.

5 RESULTS

The dynamic response from both lubrication models are compared in numerical simulations. The physical and geometric properties of each component of the mechanism are listed in Table 1.

Body	Length (m)	Mass (Kg)	Moment of Inertia (Kgm ²)
Crank	0.05	0.30	0.00010
Connecting Rod	0.12	0.21	0.00025
Slider	-	0.14	-

Table 1: Parameters of the Slider-Crank Mechanism.

The parameters used to characterize the effect of contact/friction forces and the lubrication models are listed in Table 2. The global results reported correspond to two full crank cycles obtained after the system reaches the steady-state condition, in order to ensure the inexistence of other transient effects that are not due to the joint clearance [3]. The initial conditions for all simulations were obtained from ideal mechanism in steady-state regime and the initial ec-

centricity was set as zero. The angular velocity of the crank was maintained constant at $5,000rpm$ and the radial clearance was $0,5mm$.

Bearing radius (R_i)	10.0mm	Absolute Viscosity (μ)	0.40 [Pa.s]
Restitution Coefficient (c_e)	0.90	Kinematic Viscosity (ν)	$4.54 \cdot 10^{-4}$ [m ² /s]
Friction Coefficient (c_f)	0.03	Oil Density (ρ)	880 [kg/m ³]
Contact Exponent (n)	1.50	Hydrodynamic Bearing Width (w)	0.015 [m]
Young Modulus (E)	207GPa	Maximum Step-size (Integration)	$1.00 \cdot 10^{-7}$ [s]
Poisson Ratio (ν)	0.30	Error Tolerance (Integration)	$1.00 \cdot 10^{-6}$

Table 2: Parameters used in contact/friction and lubrication models of a piston-pin system.

In Figure 4 the slider velocity with both models of lubrication are compared. The Pinkus and Sternlicht (Figure 4a) model approaches to the behaviour of an ideal joint while the proposed model (Figure 4b) shows oscillations around the ideal mechanism behaviour due to the clearance dimension and the transition between HD lubrication and Hertz contact.

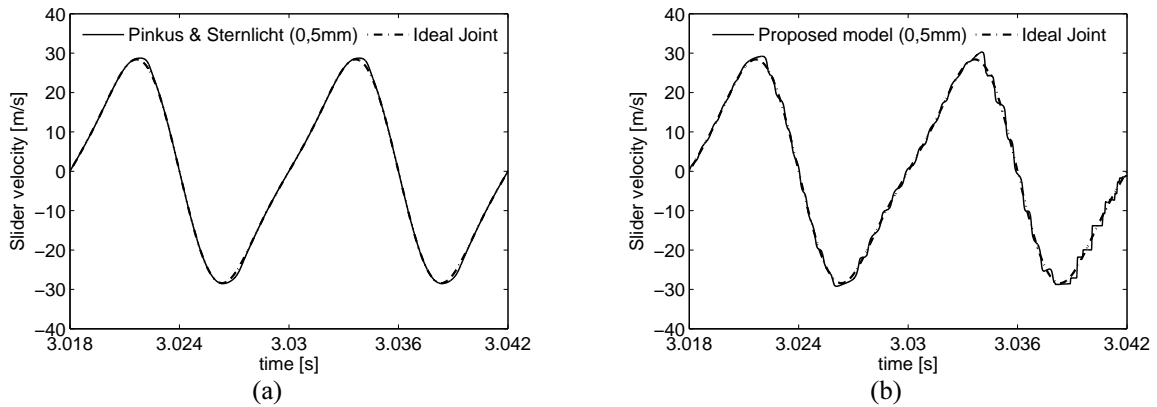


Figure 4: Slider velocity: (a) Pinkus-Sternlicht model; (b) Proposed model.

The moment applied on the crank was also investigated. The Pinkus model (Figure 5a) has a small disturbance in comparison to ideal mechanism. However, this effect is considerably stronger when the proposed model is used (Figure 5b).

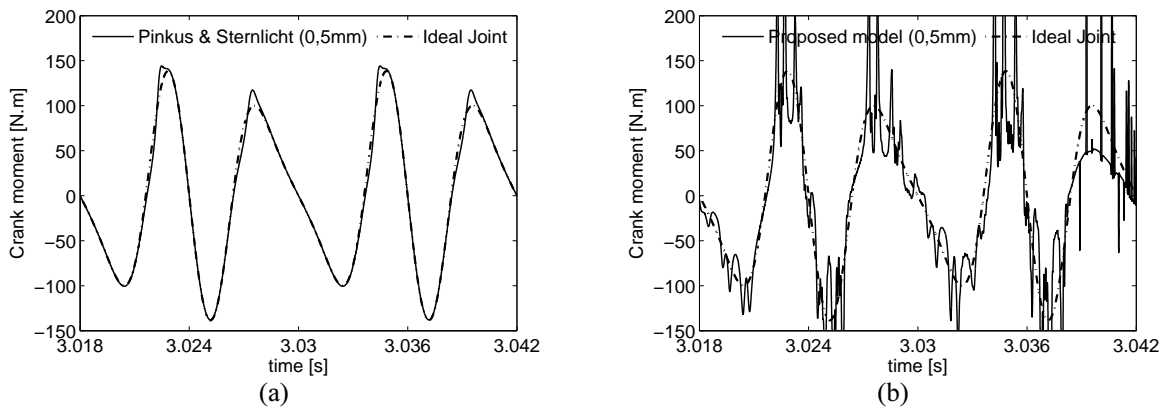


Figure 5: Crank moment: (a) Pinkus-Sternlicht model; (b) Proposed model.

It can be observed that the Pinkus model predicts a periodic journal centre trajectory (Figure 6a), without contact between the piston and the pin according to the oil film thickness

(Figure 7a) that reaches very small values, but never lets the pin goes into contact with the piston hole. The proposed model indicates the occurrence of contact when simulated in the same specified condition (Figure 6b) and the oil film thickness rarely reaches a safe value for hydrodynamic lubrication (Figure 7b).

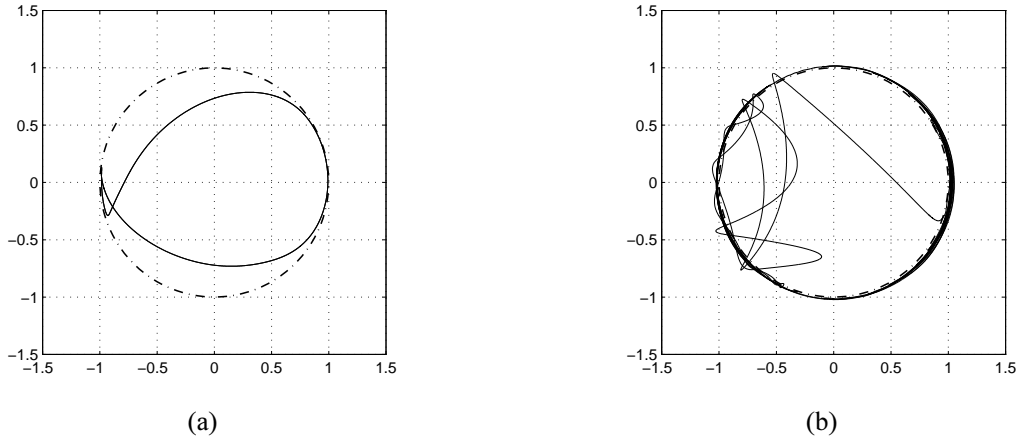


Figure 6: Journal center trajectory: (a) Pinkus-Sternlicht model; (b) Proposed model.

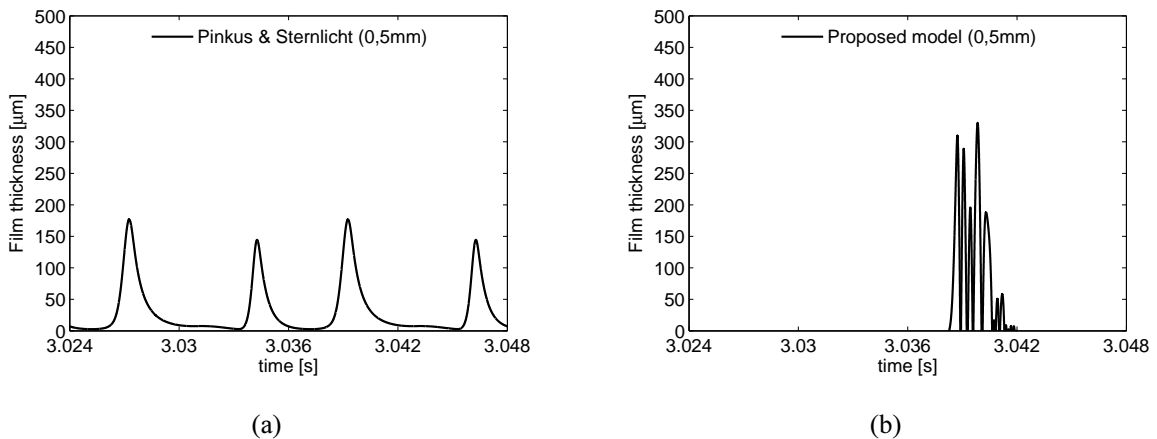


Figure 7: Oil film thickness: (a) Pinkus-Sternlicht model; (b) Proposed model.

Therefore, in the Pinkus model the pin doesn't touch the bearing wall and its lubrication is enough to guarantee safe operation. But in the proposed model [8], the forces developed are not capable of sustaining the pin in hydrodynamic lubrication, which leads to a more conservative model representing a more critical operational condition.

6 CONCLUDING REMARKS

The present paper presented the inclusion of the contact and friction forces in the dynamic model previously developed to analyze the response of the slider-crank with revolute joint clearance. Two hydrodynamic lubrication models were investigated to understand their influence in the dynamic response of this mechanism.

The results obtained showed the importance of the development of an elasto-hydrodynamic lubrication scheme to predict more accurately the complex lubrication regime present in these mechanisms.

REFERENCES

- [1] A.L. Schwab, J.P. Meijaard, P. Meijers, A comparison of revolute joint clearance model in the dynamic analysis of rigid and elastic mechanical systems. *Mechanism and Machine Theory*, **37**(9), 895–913, 2002.
- [2] P. Flores, J. Ambrósio, J.P. Claro, Dynamic analysis for planar multibody mechanical systems with lubricated joints. *Multibody Syst. Dyn.* **12**, 47–74, 2004.
- [3] P. Flores, J. Ambrósio, J. Claro, H. Lankarani, C. Koshy, A study on dynamics of mechanical systems including joints with clearance and lubrication, *Mechanism and Machine Theory*, **41**, 247-261, 2006.
- [4] P. Flores, J. Ambrósio, J. Claro, H. Lankarani, C. Koshy, Lubricated revolute joints in rigid multibody systems, *Nonlinear Dynamics*, **56**, 277-295, 2009.
- [5] Q. Tian, Y. Zhang, L. Chen, J. Yang, Simulation of planar flexible multibody systems with clearance and lubricated revolute joints. *Nonlinear Dynamics*, **60**, 489–511, 2010.
- [6] P. Ravn, S. Shivaswamy, B.J. Alshaer, H.M. Lankarani, Joint clearances with lubricated long bearings in multibody mechanical systems. *J. Mech. Des.*, **122**, 484–488, 2000.
- [7] G. B. Daniel, K. L. Cavalca, Analysis of the dynamics of a slider-crank mechanism with hydrodynamic lubrication in the connecting rod-slider joint clearance, *Mechanism and Machine Theory*, **46**, 1434-1452, 2011.
- [8] A. C. Bannwart, K. L. Cavalca, G. B. Daniel, Hydrodynamic bearings modeling with alternate motion, *Mechanics Research Communications*, **37**, 590-597, 2010.
- [9] Machado, M., Costa, J., Seabra, E., Flores, P.: The effect of the lubricated revolute joint parameters and hydrodynamic force models on the dynamic response of planar multibody systems. *Nonlinear Dynamics*, **69**, 635–654, 2012.
- [10] O. Pinkus, S.A. Sternlicht, *Theory of Hydrodynamic Lubrication*. McGraw-Hill, New York, 1961.
- [11] J. Frêne, D. Nicolas, B. Degneurce, D. Berthe, M. Godet, *Hydrodynamic Lubrication—Bearings and Thrust Bearings*. Elsevier, Amsterdam, 1997.
- [12] S. Doughty, *Mechanics of Machines*. John Wiley & Sons, 1988.
- [13] H.M. Lankarani, P.E. Nikravesh, Continuous Contact Force Models for Impact Analysis in Multibody Systems, *Nonlinear Dynamics*, **5**, 193-207, 1994.
- [14] M. Machado, P. Moreira, P. Flores, H.M. Lankarani, Compliant contact force models in multibody dynamics: Evolution of the Hertz contact theory, *Mechanism and Machine Theory*, **53**, 99–121, 2012.
- [15] J. Ambrósio, Impact of Rigid and Flexible Multibody Systems: Deformation Description and Contact Models, *Virtual Nonlinear Multibody Systems*, (Michael Valasek, Werner Schiehlen, eds.), Kluwer Academic Publishers, Dordrecht, Netherlands, 57–81, 2003.
- [16] L. F. Shampine, M. K. Gordon, *Computer Solution of Ordinary Differential Equations: The Initial Value Problem*. W.H.Freeman & Co Ltd, 1975.